A Bispecific Antibody Antagonizes Prosurvival CD40 Signaling and Promotes Vγ9Vδ2 T cell–Mediated Antitumor Responses in Human B-cell Malignancies Ⓐ🄲

Iris de Weerdt[1,2], Roeland Lameris[1], George L. Scheffer[1], Jana Vree[1], Renate de Boer[2], Anita G. Stam[1], Rieneke van de Ven[1], Mark-David Levin[3], Steven T. Pals[4,5], Rob C. Roovers[6], Paul W.H.I. Parren[6,7], Tanja D. de Gruijl[1], Arnon P. Kater[2,5], and Hans J. van der Vliet[1,6]

ABSTRACT

Novel T cell–based therapies for the treatment of B-cell malignancies, such as chronic lymphocytic leukemia (CLL) and multiple myeloma (MM), are thought to have strong potential. Progress, however, has been hampered by low efficacy and high toxicity. Tumor targeting by Vγ9Vδ2 T cells, a conserved T-cell subset with potent intrinsic antitumor properties, mediated by a bispecific antibody represents a novel approach promising high efficacy with limited toxicity. Here, we describe the generation of a bispecific Vγ9Vδ2 T-cell engager directed against CD40, which, due to its overexpression and biological footprint in malignant B cells, represents an attractive target. The CD40-targeting moiety of the bispecific antibody was selected because it can prevent CD40L-induced prosurvival signaling and reduce CD40-mediated resistance of CLL cells to venetoclax. Selective activation of Vγ9Vδ2 T cells in the presence of CD40$^+$ tumor cells induced potent Vγ9Vδ2 T-cell degranulation, cytotoxicity against CLL and MM cells *in vitro*, and *in vivo* control of MM in a xenograft model. The CD40-bispecific γδ T-cell engager demonstrated lysis of leukemic cells by autologous Vγ9Vδ2 T cells present in patient-derived samples. Taken together, our CD40 bispecific γδ T-cell engager increased the sensitivity of leukemic cells to apoptosis and induced a potent Vγ9Vδ2 T cell–dependent antileukemic response. It may, therefore, represent a potential candidate for the development of novel treatments for B-cell malignancies.

Introduction

Despite major improvements in the treatment of B-cell lineage malignancies such as chronic lymphocytic leukemia (CLL) and multiple myeloma (MM) brought about by novel agents, long-term treatment is required, eventually eliciting toxicity and resistance (1, 2). Besides targeted therapies, T cell–based therapy represents a promising antitumor approach, specifically in B-cell malignancies (3, 4). Current autologous T cell–based strategies include chimeric antigen receptor (CAR) T cells, immune-checkpoint blockade, and bispecific antibodies. The major challenges associated with these strategies include toxicity and limited response rates (complete response rate in CLL for CAR T-cell therapy: 17%–29%; for immune-checkpoint blockade: 0%; refs. 5–12). The current bispecific antibody approaches engage T cells via their CD3 antigen, which is expressed by all T cells, leading to toxicity (6–9) as well as the activation of regulatory T cells (Treg), thereby impeding effective T-cell responses (13–16).

The use of a restricted T-cell subset with inherent antitumor properties, such as Vγ9Vδ2 T cells, may circumvent these issues. Vγ9Vδ2 T cells comprise 1% to 10% of peripheral blood T cells and possess a conserved T-cell receptor (TCR) that allows MHC-independent recognition of malignant cells (17). The Vγ9Vδ2 TCR detects high expression of phosphorylated antigens in the context of butyrophilin (BTN) 3A1, which are commonly upregulated in malignant cells and can be pharmacologically increased using aminobisphosphonates (18–20). Upon activation, Vγ9Vδ2 T cells function as cytotoxic T cells that efficiently produce proinflammatory cytokines and in addition possess antigen-presenting capacity. Although we have previously shown that Vγ9Vδ2 T cells can be activated by and subsequently lyse CLL cells, the cytotoxic function of CLL-derived Vγ9Vδ2 T cells is often impaired in a CLL-mediated manner (21). Vγ9Vδ2 T cells have also been shown to be cytotoxic to MM and other malignant B cells (22). In contrast to toxicity concerns associated with pan-CD3–based strategies, clinical trials have demonstrated the safety of Vγ9Vδ2 T cell–based immunotherapy in hematologic malignancies (23–25).

CD40 is an attractive target for antibody-based antitumor strategies due to its expression on the surface of many B-cell malignancies (i.e., CLL, MM, non-Hodgkin lymphoma, Hodgkin disease, and acute lymphoblastic leukemia) and certain solid malignancies (e.g., renal cell carcinoma, breast carcinoma, melanoma, pancreatic carcinoma; refs. 26–29). CD40 functions as a costimulatory molecule on healthy B cells, and CD40 stimulation results in maturation and improved antigen-presenting function (30). Malignant B cells, including CLL cells, interact with nonmalignant immune cells within the lymph node tumor microenvironment (31), which results in inhibition of apoptosis and induction of proliferation. CD40 ligation, resulting from interactions between CLL cells and follicular T-helper cells, induces NFκB

[1]Department of Medical Oncology, Cancer Center Amsterdam, Amsterdam Infection and Immunity Institute, Amsterdam UMC, Vrije Universiteit Amsterdam, Amsterdam, the Netherlands. [2]Department of Hematology, Cancer Center Amsterdam, Amsterdam Infection and Immunity Institute, Amsterdam UMC, University of Amsterdam, Amsterdam, the Netherlands. [3]Department of Internal Medicine, Albert Schweitzer Hospital, Dordrecht, the Netherlands. [4]Department of Pathology, Cancer Center Amsterdam, Amsterdam UMC, University of Amsterdam, Amsterdam, the Netherlands. [5]Lymphoma and Myeloma Center Amsterdam (LYMMCARE), Amsterdam, the Netherlands. [6]Lava Therapeutics, Utrecht, the Netherlands. [7]Department of Immunohematology and Blood Transfusion, Leiden University Medical Center, Leiden, the Netherlands.

Corresponding Author: Hans J. van der Vliet, Lava Therapeutics, Yalelaan 60, 3584 CM, Utrecht, the Netherlands. E-mail: h.vandervliet@lavatherapeutics.com or jj.vandervliet@amsterdamumc.nl

and mTOR activation, resulting in increased expression of antiapoptotic Bcl-2 family members and resistance to apoptosis-inducing agents such as fludarabine and the Bcl-2 antagonist venetoclax (32–35). Although CD40 stimulation has been reported to induce apoptosis of MM cells, it also provides tumor support by stimulating MM cell proliferation and promoting bone marrow (BM) homing (36, 37). Antagonistic CD40 antibodies that aim to disrupt CD40 signaling therefore hold therapeutic potential. As a monotherapeutic agent, the monovalent CD40-specific antagonistic antibody lucatumumab has demonstrated limited activity in CLL and MM (38, 39).

We set out to develop a bispecific antibody that antagonizes CD40 stimulation and simultaneously activates Vγ9Vδ2 T cells upon binding to CD40. The bispecific antibody was composed of two variable antigen-binding fragments derived from heavy chain–only antibodies (VHH; ref. 40). The low immunogenicity risk profile, as well as relative ease and low cost of production, support the use of the bispecific VHH format. Here, we describe the generation of a CD40-specific Vγ9Vδ2 T-cell engager, which prevented CD40/CD40L-induced prosurvival signaling and activated Vγ9Vδ2 T cells from healthy controls (HC) and leukemic patients to induce lysis of CLL and MM cells *in vitro* and in *in vivo* models.

Materials and Methods

Patient and healthy donor material

Peripheral blood (PB) samples were taken from patients with CLL, as defined by iwCLL criteria, who had not been previously treated, between 2014 and 2019. Buffy coats from blood donors (age ≥60 years) obtained from Sanquin Blood Supply (Amsterdam, the Netherlands) between 2015 and 2019 were used for HCs (**Table 1**). PB mononuclear cells (PBMC) were isolated by Ficoll (VWR) density gradient centrifugation, frozen in Iscove's Modified Dulbecco's Medium (IMDM; 12440-053, Thermo Fisher Scientific) supplemented with 10% DMSO (VWR), 23% fetal calf serum (FCS; F7524), 0.05 mmol/L β-mercaptoethanol (M6250, both Merck), 200 mmol/L L-glutamine (25030-123), and 10 kU/mL penicillin/streptomycin (15140-122, both Thermo Fisher Scientific) and stored in liquid nitrogen. Mononuclear cells from the BM of MM patients ($n = 6$, median age 53.5 years; range, 34–62) were isolated similarly and cryopreserved in FCS supplemented with 10% DMSO. The presence of monoclonal B-cell lymphocytosis was excluded in HCs by CD5, CD19, κ, and λ immunophenotyping. Healthy B cells were obtained from HC PBMCs by CD19 selection (magnetic microbeads, 130-050-301, Miltenyi Biotec). The study was approved by the institutional review boards of the Academic Medical Center and VU Medical Center. Written informed consent from all subjects was obtained in accordance with the Declaration of Helsinki.

Vγ9Vδ2 T cells and cell lines

Expanded Vγ9Vδ2 T cells were generated as described previously (41). In short, Vδ2$^+$ T cells were isolated from HC PBMCs using FITC-conjugated anti-Vδ2 TCR (Supplementary Table S1) in combination with anti-mouse IgG microbeads (Miltenyi Biotec) and cultured weekly with irradiated feeder mix consisting of PBMCs from two HCs (1×10^6 cells/mL from each donor), JY cells (1×10^5 cells/mL), IL7 (10 U/mL), IL15 (10 ng/mL, R&D Systems), and PHA (R30852801, Thermo Fisher Scientific). Cells were expanded for at least two cycles prior to their use, and purity of Vγ9Vδ2 T cells was maintained at >90%.

All culture media were supplemented with 10% FCS, 0.05 mmol/L β-mercapto-ethanol, 200 mmol/L L-glutamine, and penicillin/strep-

Table 1. CLL patient characteristics.

N	44
Age in years	69.5 (range, 39–89)
Sex, % female	36.4
IGHV, % M-CLL	55.2 (for 29 known)
Rai, % stage 0	67.9 (for 28 known)
ALC $\times 10^9$/L	66.0 (13.1–422)

Note: Data presented as a percentage or median (range).
Abbreviations: ALC, absolute leukocyte count; M-CLL, CLL cells with a mutated IGHV status.

tomycin (10 kU/mL). HEK293T cells (ATCC), either wild-type or transfected with CD40 as described below, were grown in supplemented Dulbecco's Modified Eagle Medium (41965-039; Thermo Fisher Scientific). HEK293E-253 (ATCC) cells were grown in FreeStyle 293 Expression medium (Thermo Fisher Scientific). The CLL cell line CII (kind gift from Professor T. Stankovic, Institute of Cancer and Genomic Sciences, University of Birmingham, Birmingham, UK) and MM cell line MM.1s, either wild-type or stably transduced with CD1d-mCherry (ref. 42; kind gift from Dr. R. Groen, Amsterdam UMC, Vrije Universiteit, Amsterdam, the Netherlands), were cultured in supplemented Roswell Park Memorial Institute 1640 medium (52400-025; Thermo Fisher Scientific). NIH/3T3 fibroblasts (ATCC), either wild-type (3T3) or stably transfected with a plasmid encoding human CD40L (3T40L; ref. 43), were cultured in supplemented IMDM. Authentication of human cell lines was performed using short-tandem repeat analysis (DC6531, Promega). All cell lines were used within 3 months of thawing and checked for *Mycoplasma* using PCR at least every 3 months.

Flow cytometry

Cells were stained with antibodies, and viability dyes were listed in Supplementary Table S1. Cytofix/Cytoperm reagent (BD Biosciences) was used for detection of intracellular cytokines, and the FoxP3 staining buffer set (Thermo Fisher Scientific) was used for detection of intracellular Bcl-xL. Samples were measured on an LSRFortessa or FACSCanto cytometer and analyzed with FlowJo MacV10 (all BD Biosciences; gating strategy in Supplementary Information).

VHH generation

Llama immunization and construction of the VHH phage library

The Vδ2-TCR chain-specific VHH 5C8 was previously generated (44), and CD40-specific VHHs were generated similarly. Two llamas (*Lama glama*) were immunized subcutaneously six times with 50×10^6 MUTZ-3 dendritic cells (DC; DSMZ; ref. 45), with a 1-week interval.

RNA was isolated from PB lymphocytes obtained 1 week after the last immunization, reverse-transcribed into cDNA, and used for Ig-heavy chain-encoding gene amplification (46). Phage libraries were constructed by ligation of VHH-encoding genes into the phagemid vector pUR8100 containing a Myc- and His6-tag encoding fragment (kind gift from Dr. M. El Khattabi, QVQ, Utrecht, the Netherlands) and subsequent transformation into *Escherichia coli* TG1 for display on filamentous bacteriophage. Llama immunization and construction of the VHH phage library was performed at Eurogentec in collaboration with QVQ in accordance with institutional and international guidelines.

Enrichment and selection of CD40-specific VHHs

To enrich for phages displaying CD40-specific VHHs, multiple selection rounds were performed. 96-well flat-bottom plates were coated with IgG1-Fc–tagged human CD40 (2.25 µg/mL; 71174, BPS Bioscience). Phages were blocked with PBS (Fresenius Kabi) containing 1% bovine serum albumin (Sigma-Aldrich), 1% milk (Nutrilon), 0.05% Tween 20 (Merck), and human IgG (0.625 mg/mL, Thermo Fisher Scientific) and then allowed to bind to the CD40-coated plates for 90 minutes at 37°C. Eluted phages (150 µL) were used to infect exponentially growing *E. coli* TG1 (600 µL). After two rounds, ELISA-based screening was performed to select for binding to human CD40, but not human Ig. For this, plates were coated either with IgG1-Fc–tagged human CD40 or human IgG1 and incubated with periplasmic extracts from the transformed TG1. Bound extracts were detected by sequential incubation with mouse-derived anti-Myc tag (05-274, Merck) and HRP-conjugated rabbit-derived anti-mouse IgG (Cell Signaling Technology). DNA sequencing was performed on 22 clones that bound to human CD40 but not human Ig, as well as two negative-control clones that did not bind to CD40, translated to amino acid sequences using the ExPASy Translate tool and aligned using MUSCLE. DNA sequence analysis of selected clones demonstrated three different CD40-specific VHH sequences termed V12, V15, and V19 (Supplementary Table S2).

VHH production

Monovalent VHH

Gene segments encoding the three selected VHHs and a Myc- and His6-tag were recloned into the pcDNA5 vector (Invitrogen). Plasmid (15 µg), GENIUS DNA transfection reagent (Westburg), and Opti-MEM (Thermo Fisher Scientific) was used to transfect 80% confluent HEK293T cells in T225 flasks for 15 minutes at room temperature. VHH protein (V12t, V15t, and V19t) was purified from the HEK293T supernatant using fast protein liquid chromatography with an ÄKTApurifier (GE Healthcare). First, size exclusion was performed a HiPrep 26/10 desalting column (10 mL sample injection volume, CP limit 1.5 kPa, 5 mL/min; buffer: 500 mmol/L sodiumchloride, 20 mmol/L sodiumphosphate, 20 mmol/L imidazole) followed by washing the column with 70 mL buffer. Subsequently, nickel-based His-tag selection was performed in a 1 mL HisTrap column (30 mL sample injection volume, CP limit 0.7 kPa, 5 mL/min; both columns GE Healthcare) and imidazole-based elution (buffer: 500 mmol/L sodiumchloride, 20 mmol/L sodiumphosphate, and 500 mmol/L imidazole) in 30 eluate fractions of 1 mL. In this manner, three monovalent CD40-specific VHHs were retrieved (V12t, V15t, and V19t), in which "t" indicates the presence of an Myc and His6 tag.

Bispecific VHH

To generate bispecific VHH constructs, V12-5C8t, V15-5C8t, and V19-5C8t, the anti-Vδ2-TCR VHH 5C8 (C-terminal) was joined to the anti-CD40 VHHs (N-terminal) with a Gly₄Ser-linker. The bispecific VHHs, containing a Myc and His6 tag, were produced by HEK293T transfection as described above. VHH protein was purified from the supernatant using immobilized ion affinity chromatography on Talon resin (Clontech) followed by elution with 250 mmol/L and dialysis against PBS using 10K molecular weight cutoff Slide-A-Lyzer dialysis cassettes (Thermo Fisher Scientific).

Generation of V19S76K-5C8

A glycosylation site in framework region 3 of the V19t VHH was identified, after which a new VHH (V19S76K) was produced and purified in which the relevant serine was altered into a lysine. This variant retained its binding capacity to CD40-expressing cells. Tagless bispecific V19S76K-5C8 VHH, hereafter referred to as V19-5C8, was constructed analogous to the bispecific VHH. VHH protein was generated by U-protein Express, after transfection into HEK293E-253 cells. V19-5C8 protein was purified from the supernatant using fast protein liquid chromatography with an ÄKTAexplorer (GE Healthcare). VHH was bound to a 35 mL rmp protein A column (GE Healthcare) at 11°C, followed by washing the column with PBS and acid-based elution (buffer: 20 mmol/L citrate, 150 mmol/L sodiumchloride, pH 3.0). Eluate fractions (5 mL) were collected in 1 mL alkaline buffer (1 mol/L dipotassium phosphate, pH 8.0) for neutralization to pH 7. The column was regenerated with 50 mmol/L sodium hydroxide containing 1 mol/L sodium chloride and equilibrated in PBS. The purification was repeated five times. VHH-containing fractions were concentrated using a Vivaspin20 10kDa molecular weight cutoff filter (GE Healthcare) and further purified by gefiltration using a Superdex 200 column (GE Healthcare) equilibrated with PBS.

VHH integrity

VHH integrity and purity were confirmed by Coomassie blue staining in NuPAGE gels. VHH was quantified using a Nanodrop spectrophotometer.

VHH binding

To assess binding, cells were incubated with the indicated concentrations of VHH for 30 minutes at 37°C. Bound VHH was detected by sequential incubation with mouse anti-Myc tag and Alexa Fluor (AF) 488–conjugated goat anti-mouse antibodies for 20 minutes at 4°C (Supplementary Table S1). Bound tagless VHH was detected with FITC-conjugated anti-llama antibodies. VHH binding was determined using flow cytometry and quantified by geometric mean fluorescence intensity.

Analysis of agonistic and antagonistic effects of CD40-specific VHHs

To assess whether VHH binding to CD40 led to CD40 stimulation, 300,000 primary CLL PBMCs (>90%, CD5⁺CD19⁺) were cultured for 48 hours in the presence of 10 nmol/L, 100 nmol/L, or 1 µmol/L VHH, medium control, or recombinant multimeric CD40 ligand (100 ng/mL, Bioconnect) as indicated, and phenotyped by flow cytometry. Relative data were calculated by dividing experimental conditions by control condition without VHH *100.

To test whether the VHH antagonized CD40 stimulation, primary CLL PBMCs were preincubated with VHH or medium control for 30 minutes at 37°C and subsequently cultured for 48 hours in the presence of recombinant multimeric CD40L (100 ng/mL). After 48 hours, cells were phenotyped by flow cytometry as described above. Relative data were calculated by dividing experimental conditions by control condition with recombinant multimeric CD40L in the absence of VHH *100.

Cytokine and degranulation assays

Expanded Vγ9Vδ2 T cells (50,000) were incubated with the indicated concentrations of VHH or medium control for 30 minutes at 37°C. Subsequently, Vγ9Vδ2 T cells were cocultured with CLL-derived CII cells for 4 hours in a 1:1 ratio in the presence of Brefeldin A (10 µg/mL; Thermo Fisher Scientific), GolgiStop (7% v/v), and anti-CD107a (both BD Biosciences). In the assays with autologous Vγ9Vδ2 T cells, CLL PBMCs or MM BM cells were cultured overnight with

10 nmol/L VHH or medium control in the presence of Brefeldin A, GolgiStop, and anti-CD107a as above. Prior to culture, CLL PBMCs were partially depleted of CD19$^+$ cells using magnetic beads (130-050-301, Miltenyi Biotec; after depletion ±50% of cells were CD19$^+$). Cytokine production and degranulation were then determined by flow cytometry as described above.

Cytotoxicity assays

For cytotoxicity assays, target cells (CII, primary CLL, MM.1s, HEK293T cells as indicated) were preincubated with the indicated concentration of VHH or medium control for 30 minutes at 37°C and then cocultured overnight with expanded Vγ9Vδ2 T cells in a 1:1 (Vγ9Vδ2 T-cell:target cell) ratio, unless otherwise indicated. Target cells were identified by mCherry expression (MM.1s.mCherry/luc) or prior carboxyfluorescein succinimidyl ester (CFSE; Thermo Fisher Scientific) labeling in all other cell lines and primary CLL cells (>90%, CD5$^+$CD19$^+$). The percentage of viable cells was determined using MitoTracker Orange (25-minute incubation at 37°C) and To-pro-3 (10-minute incubation at room temperature; both Thermo Fisher Scientific) by flow cytometry.

For cytotoxicity assays performed with patient-derived Vγ9Vδ2 T cells, CD3$^+$ cells were enriched by magnetic bead selection (130-050-101, Miltenyi Biotec; ≥90% purity). PBMCs were preincubated with

10 nmol/L VHH or medium control for 30 minutes at 37°C and cultured overnight with purified CD3$^+$ cells from the same patient in a 5:1 or 20:1 (CD3$^+$:PBMC) ratio. For cytotoxicity assays with primary MM cells as target cells, BM was preincubated with 10 pmol/L or 10 nmol/L VHH or medium control for 30 minutes at 37°C and cultured overnight with expanded Vγ9Vδ2 T cells in a 1:1 (Vγ9Vδ2:plasma cell) ratio. In assays with patient-derived Vγ9Vδ2 T cells as effector cells and assays with primary MM cells as target cells, viable cells were quantified by fluorescently labeled antibodies and viability dyes (Supplementary Table S1) in combination with counting beads (01-1234-42, Thermo Fisher Scientific).

Expansion assays

For expansion assays, 1×10^6 PBMCs were cultured with 10 nmol/L VHH or medium control in the presence of IL2 (50 IU/mL, AF-2002–02, Bioconnect) for 1 week, after which the percentage of Vγ9Vδ2 T cells was determined by flow cytometry.

In vivo studies

Immunodeficient NOD *SCID* gamma (NSG) mice ages 16 to 26 weeks were obtained from Charles River. Mice were housed in isolators under pathogen-free conditions and randomly divided in three control groups (group 1: PBS and PBS; group 2: PBS and Vγ9Vδ2
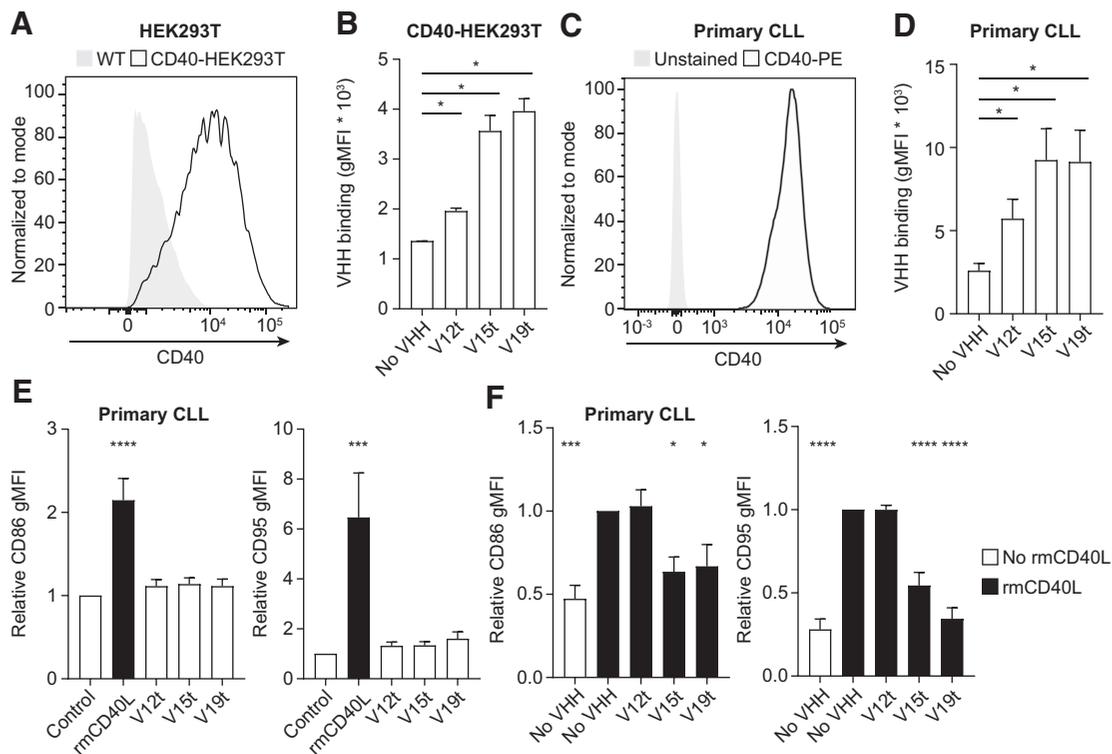

Figure 1.
Selection of CD40-specific VHHs. **A,** CD40 expression on wild-type (WT; gray, filled histogram) and CD40-transfected (black, open histogram) HEK293T cells. **B,** CD40 specificity of VHH binding. WT and CD40-transfected HEK293T cells were incubated with V12t, V15t, V19t (1 μmol/L), or medium control, and VHH binding was measured by flow-cytometric detection of the Myc tag. Representative histograms of three experiments. gMFI, geometric mean fluorescence intensity. **C,** CD40 expression on primary CLL cells. Representative histograms of five experiments. **D,** Binding of CD40-specific VHHs (1 μmol/L) to primary CLL cells as in **B** (*n* = 5). **E,** Primary CLL PBMCs were cultured with V12t, V15t, V19t (all 1 μmol/L), recombinant multimeric CD40L (100 ng/mL), or medium control and analyzed for CD86 and CD95 expression after 48 hours (*n* = 5). **F,** Primary CLL PBMCs were preincubated with V12t, V15t, V19t (all 1 μmol/L), or medium control for 30 minutes, and then cultured with recombinant multimeric CD40L (100 ng/mL) for 48 hours and analyzed for CD86 and CD95 expression after 48 hours (*n* = 9). Data, mean and SEM. *, $P < 0.05$; ***, $P < 0.001$; ****, $P < 0.0001$. For **D**, repeated-measures one-way ANOVA followed by Dunnett *post hoc* test compared with no VHH; for **E** and **F**, one-way ANOVA followed by Dunnett *post hoc* test compared with medium control.

de Weerdt et al.

T cells; group 3: VHH and PBS) and one experimental group (group 4: VHH and Vγ9Vδ2 T cells). On day −1, mice were irradiated (2 Gy) and, on day 0, injected intravenously with 2.5×10^6 MM.1s. mCherry/luc cells. On days 7, 14, and 21, mice received either PBS or 1×10^7 expanded human Vγ9Vδ2 T cells intravenously. From day 7, mice also received PBS or V19-5C8 (100 μg per mouse) intraperitoneally biweekly. Mice were weighed weekly, and PB samples were taken at days 20 and 50. Mice were euthanized in case of severe weight loss (>10% of initial body weight), paralysis, or other symptoms of severe disease burden. PB, BM, and plasmacytomas were collected from mice. Animal experiments were approved by the Dutch Central Authority for Scientific Procedures on Animals (CCD) and handled in accordance with institutional and international guidelines.

Statistical analyses

Specific lysis was calculated as: (% cell death in treated cells) − (% cell death in untreated cells)/(% viable cells in untreated cells) × 100. Data were analyzed using one-way analysis of variance (ANOVA; followed by Dunnett *post hoc* test), two-way ANOVA (followed by Tukey, Šidák, or Dunnett *post hoc* test as appropriate), Mantel–Cox log-rank test (followed by Holm–Šidák *post hoc* test), or nonlinear regression analysis as indicated with significance set at $P < 0.05$ using GraphPad Prism v7.

Results

Identification of monovalent CD40-specific VHHs

To generate CD40-specific VHHs, two *Lama glamas* were immunized six times (weekly intervals) with $CD40^+$ MUTZ-3 DCs. Three putative CD40-heavy chain–only binding domains were identified through phage display and ELISA-based screening using a CD40–IgG Fc fusion protein. Wild-type ($CD40^-$) HEK293T cells and HEK293T cells stably transfected to express CD40 (**Fig. 1A**) were then used to confirm binding specificity of these three distinct VHHs, termed V12t, V15t, and V19t. None of the CD40-specific VHHs bound to wild-type HEK293T cells, but all bound to $CD40^+$ HEK293T cells, with the highest binding intensity observed for V15t and V19t (**Fig. 1B**). Primary CLL cells homogeneously expressed CD40 on the cell surface (**Fig. 1C**). All three VHHs bound to CLL cells, although V15t and V19t had a higher binding intensity than V12t ($n = 5$; **Fig. 1D**).

To test whether binding of the VHHs activated CD40 signaling, CLL cells were cultured for 48 hours with the CD40-specific VHHs. Whereas the positive control, recombinant multimeric CD40L (rmCD40L), increased expression of the costimulatory molecule CD86 and the death receptor CD95 on CLL cells, these effects were not seen with any of the CD40-specific VHHs (**Fig. 1E**). Next, we evaluated whether the CD40-specific VHHs could prevent CD40L–-CD40 interactions. As expected, rmCD40L enhanced upregulation of both CD86 and CD95, which was averted by both V15t and V19t but not by V12t (**Fig. 1F**). Taken together, we generated and identified three monovalent VHHs that specifically bound to surface-expressed CD40, none of which exerted agonistic effects and two of which antagonized the prosurvival stimulus that is provided to CLL cells by CD40 stimulation.

The bispecific anti-CD40-Vδ2 VHHs induce target cell lysis

We then set out to construct an anti-CD40–directed bispecific Vγ9Vδ2 T-cell engager by joining each of the monovalent

CD40-specific VHHs (N-terminal) to the previously generated Vδ2-specific VHH 5C8 (ref. 44; C-terminal) with a Gly_4–Ser linker. Specific binding to CD40 was retained by all three VHHs in the bispecific format (**Fig. 2A**).

Subsequently, we assessed whether the bispecific anti-CD40-Vδ2 VHHs induced Vγ9Vδ2 T cell–mediated cytotoxicity of $CD40^+$ tumor cells. Healthy donor–derived Vγ9Vδ2 T cells did not induce appreciable lysis of the CLL-derived cell line CII, which has high expression of CD40 (Supplementary Fig. S1A; **Fig. 2B**). The addition of the bispecific anti-CD40-Vδ2 VHHs, especially V15-5C8t and V19-5C8t, induced tumor cell death in a dose-dependent manner. After a 4-hour coculture with primary CLL cells, Vγ9Vδ2 T cells induced cell death in 16.1% (±3.1) of the CLL cells (background viability 84.3%–85.0%; **Fig. 2C**). This was again enhanced by V12-5C8t (100 nmol/L; 45.3% ± 4.0%), in particular by V15-5C8t (100 nmol/L; 70.5% ± 7.3%) and V19–5C8t (100 nmol/L; 68.5% ± 7.9%).

High affinity and potency of bispecific anti-CD40-Vδ2 VHH

For subsequent experiments and a more in-depth characterization, we selected V19-5C8 because both the V19t monovalent- and bispecific V19-5C8t–based VHH performed slightly better in terms of blocking CD40 stimulation and inducing cytotoxicity. The presence of a glycosylation site in framework region 3 of V19 prompted generation of a VHH in which a serine residue (at position 76) was modified into a lysine. This alteration did not significantly change the binding characteristics to CD40 [K_D 17.8 nmol/L (V19t) vs. 16.4 nmol/L (V19S76Kt), Supplementary Fig. S1B]. The affinity of the modified bispecific anti-CD40-Vδ2 VHH, V19-5C8, binding to Vγ9Vδ2 T cells and CII cells was assessed by flow cytometry. Binding of the bispecific VHH to Vγ9Vδ2 T cells was detectable at 100 pmol/L, with maximum binding reached at 10 nmol/L (K_D 1.2 nmol/L; **Fig. 3A**). The bispecific VHH bound to $CD40^+$ cells with an affinity of K_D 10.9 nmol/L.

Addition of the bispecific VHH induced an activated phenotype in Vγ9Vδ2 T cells exposed to $CD40^+$ target cells, as measured by upregulation of CD69 expression [geometric mean fluorescence intensity (MFI) 1,001 ± 183.0 without bispecific VHH vs. 1,337 ± 193.3 with bispecific VHH, $P = 0.049$]. Upon coculture with $CD40^+$ target cells alone, Vγ9Vδ2 T cells did not produce detectable IFNγ or TNF (**Fig. 3B**). The addition of the bispecific VHH induced effector-type cytokine production by the majority of Vγ9Vδ2 T cells at picomolar concentrations (EC_{50} 7.1 and 4.5 pmol/L, for IFNγ and TNF, respectively). To a lesser degree, Vγ9Vδ2 T cells also produced IL2. Vγ9Vδ2 T cells exert antitumor activity through the release of granzymes and perforin. The CII target cells alone did not elicit degranulation of Vγ9Vδ2 T cells, which did occur upon addition of the bispecific VHH (EC_{50} 3.6 pmol/L; **Fig. 3B**). The bispecific VHH enhanced lysis of both $CD40^+$ CLL-derived and MM-derived cell lines at similar concentrations (EC_{50} 9.1 and 5.3 pmol/L; **Fig. 3C**; Supplementary Fig. S1C for CD40 expression on MM.1s cells). An irrelevant control bispecific VHH, consisting of the same Vδ2-specific VHH (5C8) coupled to a CD1d-specific VHH (1D7) did not induce lysis of the MM-derived cell line. The bispecific VHH did not induce lysis in the absence of Vγ9Vδ2 T cells, demonstrating that the cytotoxicity was mediated by Vγ9Vδ2 T cells. The bispecific VHH evoked cytotoxicity in a CD40-specific manner because it augmented the lysis of CD40-transfected HEK293T cells, but not of its $CD40^-$ parental cell line (**Fig. 3D**). Taken together, the bispecific anti-CD40-Vδ2 VHH, V19-5C8, potently activated Vγ9Vδ2 T cells and induced cell death of a CLL and MM cell line in a CD40-specific manner.

Figure 2.
The bispecific anti-CD40-Vδ2 VHHs induce target cell lysis. **A,** Binding of bispecific anti-CD40-Vδ2 VHHs. CD40-transfected or wild-type (WT) HEK293T cells were incubated with V12-5C8t, V15-5C8t, V19-5C8t (1 μmol/L), or medium control, and VHH binding was measured by flow-cytometric detection of the Myc tag. Representative histograms of two experiments. **B,** Specific lysis of the CII cell line after overnight culture with healthy donor–derived Vγ9Vδ2 T cells in a 1:2 effector:target ratio in the presence of the indicated concentrations of the bispecific anti-CD40-Vδ2 VHHs V12-5C8t, V15-5C8t, or V19-5C8t ($n = 5$). bsVHH, bispecific VHH. **C,** Specific lysis of primary CLL cells after overnight culture with healthy donor–derived Vγ9Vδ2 T cells in a 1:1 ratio in the presence of the indicated concentrations of the bispecific anti-CD40-Vδ2 VHHs V12-5C8t, V15-5C8t, or V19-5C8t ($n = 3$). Specific lysis was calculated by correcting for background cell death in conditions without Vγ9Vδ2 T cells. Data, mean and range, with the line depicting a nonlinear regression curve. **B** and **C,** Nonlinear regression analysis; "0" value entered as 10^{-4}.
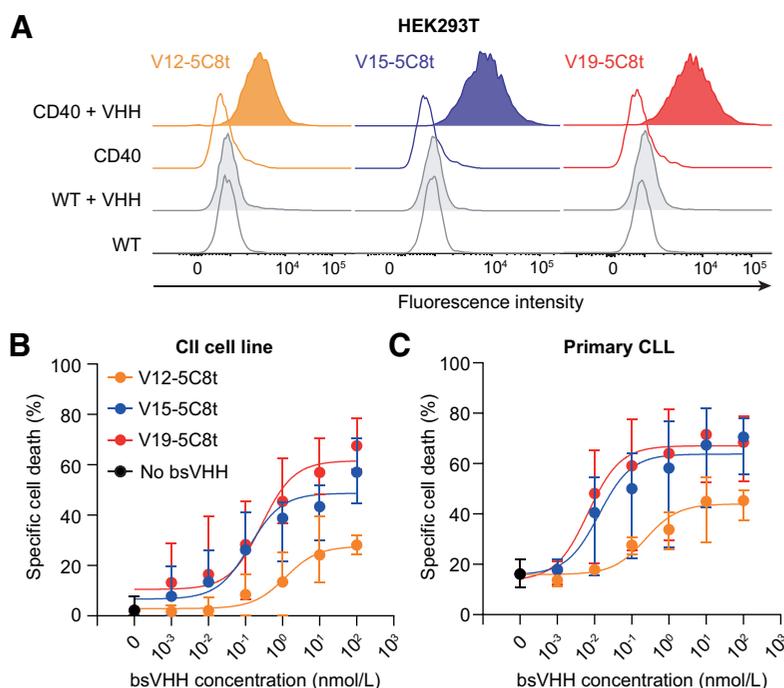

The bispecific anti-CD40-Vδ2 VHH is active against primary CLL

Next, we evaluated the activity of the bispecific VHH against primary leukemic cells. The bispecific VHH did not induce target cell death directly (specific cell death 2.0% ± 1.0%), but increased the lysis of primary CLL cells by Vγ9Vδ2 T cells (70.5% ± 4.4% with 100 nmol/L; **Fig. 4A**). CLL cells with a mutated IGHV status (M-CLL) had a comparable CD40 expression and were equally sensitive to the bispecific VHH-induced cytotoxicity as those with an unmutated IGHV status (U-CLL; Supplementary Fig. S2A). Because CD40

Figure 3.
The bispecific anti-CD40-Vδ2 VHH has a high binding affinity and potently activates Vγ9Vδ2 T cells. **A,** Binding of the bispecific anti-CD40-Vδ2 VHH to Vγ9Vδ2 T cells and CD40^{+} cells. Healthy donor–derived Vγ9Vδ2 T cells (green, $n = 3$ donors) or CII cells (black, triplicate) were incubated with the indicated concentrations of V19-5C8, and VHH binding was measured by flow-cytometric detection of anti-llama IgG heavy- and light-chain antibodies; geometric mean fluorescence plotted. bsVHH, bispecific VHH; gMFI, geometric mean fluorescence intensity. **B,** Activation of Vγ9Vδ2 T cells by the bispecific anti-CD40-Vδ2 VHH. Healthy donor–derived Vγ9Vδ2 T cells and CII target cells were cultured in a 1:1 ratio with V19-5C8 for 4 hours in the presence of Brefeldin A, GolgiStop, and anti-CD107a to measure IFNγ, TNF, and IL2 production and degranulation by flow cytometry ($n = 3$). **C,** Specific lysis of CII or MM.1s target cells after overnight culture with healthy donor–derived Vγ9Vδ2 T cells in a 1:1 ratio in the presence of V19-5C8 (circles) or the irrelevant bispecific anti-CD1d-Vδ2 VHH 1d7-5C8 (squares; all $n = 4$). Specific lysis was calculated by correcting for background cell death in conditions with Vγ9Vδ2 T cells, without bispecific VHH. **D,** Specific lysis of wild-type (WT) or CD40-transfected HEK293T cells as in **C** ($n = 4$). Specific lysis was calculated by correcting for background cell death in conditions without Vγ9Vδ2 T cells. Data, mean and range, with the line depicting a nonlinear regression curve (**A–C**) or mean and SEM (**D**). ****, $P < 0.0001$. For **A–C**, nonlinear regression analysis; for **D**, mixed-effects analysis with Šidák post hoc test comparing CD40-transfected versus WT.
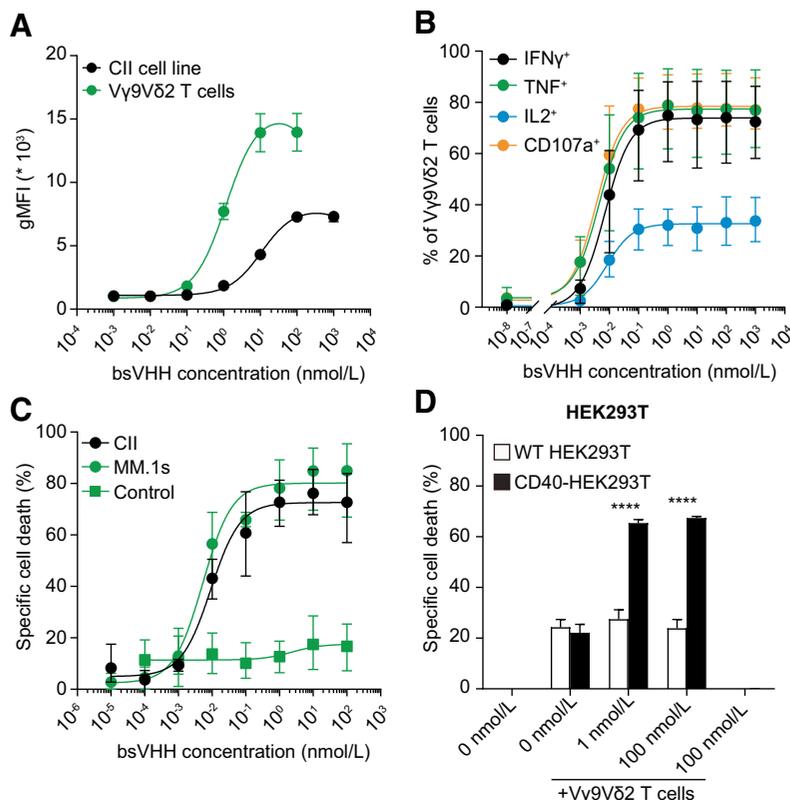
de Weerdt et al.
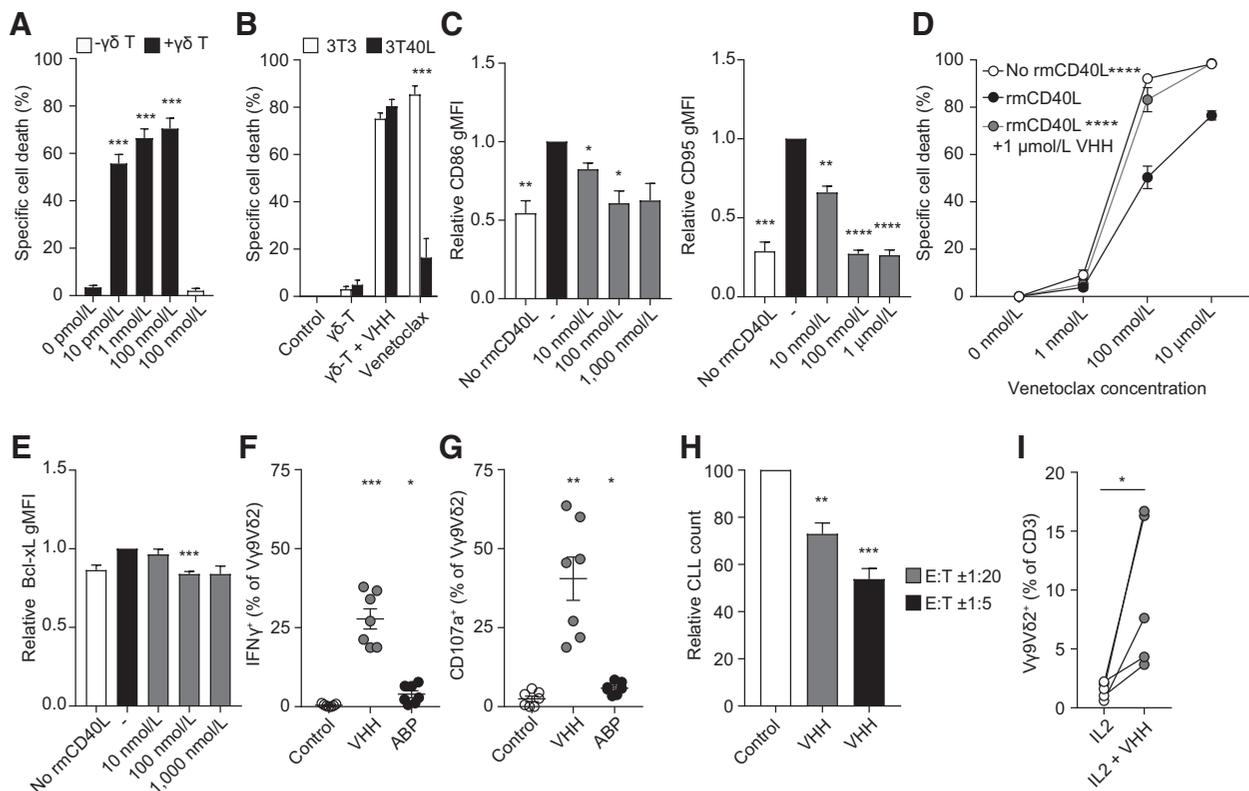
Figure 4.
The bispecific anti-CD40-Vδ2 VHH activates Vγ9Vδ2 T cells from CLL patients and induces autologous tumor lysis. **A,** Specific lysis of primary CLL cells after overnight culture with healthy donor–derived Vγ9Vδ2 T cells in a 1:1 ratio in the presence of V19-5C8 ($n = 10$). **B,** CLL PBMCs were cultured on irradiated 3T3 or CD40L^{+} 3T40L fibroblasts for 72 hours. Specific cell death of harvested CLL PBMCs after subsequent overnight culture with healthy donor–derived Vγ9Vδ2 T cells (1:1 ratio), healthy donor–derived Vγ9Vδ2 T cells and V19-5C8 (1:1 ratio, 100 nmol/L), venetoclax (10 nmol/L), or medium control ($n = 3$). **C–E,** CLL PBMCs were preincubated with 10, 100, or 1,000 nmol/L V19-5C8 or medium control for 30 minutes and then cultured in the presence of recombinant multimeric CD40L (100 ng/mL) for 48 hours. **C,** CD86 and CD95 expression after 48 hours ($n = 6$). **D,** Specific cell death after subsequent culture with the indicated concentrations of venetoclax for 24 hours ($n = 6$). **E,** Bcl-xL expression after 48 hours ($n = 3$). **F** and **G,** PBMCs from CLL patients were enriched for T cells by depletion of CD19^{+} CLL cells and then cultured with CD19^{+} CLL cells in a 1:1 ratio with V19-5C8 (10 nmol/L), aminobisphosphonates (ABP; 25 μmol/L pamidronate), or medium control in the presence of Brefeldin A, GolgiStop, and anti-CD107a to measure IFNγ production (**F**) and degranulation (**G**) by flow cytometry ($n = 7$). **H,** Lysis of primary CLL cells by autologous Vγ9Vδ2 T cells. CD3^{+} cells were isolated from CLL PBMCs and cultured with total CLL PBMCs in a 5:1 (CD3:PBMC; ±1:20 Vδ2:PBMC ratio; range, 1:10–1:24) or 20:1 (CD3:PBMC; ±1:3 Vδ2:PBMC ratio; range, 1:3–1:6) ratio with V19-5C8 (10 nmol/L) or medium control. Live CLL cells were quantified by flow cytometry using counting beads ($n = 5$). **I,** Percentage Vγ9Vδ2 T cells after PBMCs were cultured with IL2 (50 IU/mL) or IL2 and the bispecific VHH V19-5C8 (10 nmol/L) for 1 week ($n = 5$). Data, mean and SEM. *, $P < 0.05$; **, $P < 0.01$; ***, $P < 0.001$; ****, $P < 0.0001$. For **A**, **C**, and **E–H**, repeated-measures one-way ANOVA followed by Dunnett *post hoc* test compared with conditions without VHH; for **B**, two-way ANOVA followed by Šidák *post hoc* test comparing each treatment condition between the CLL groups; for **D**, two-way ANOVA followed by Dunnett *post hoc* test comparing conditions to medium control; and for **I**, paired *t* test.

stimulation decreases the apoptotic sensitivity of CLL (32, 35), we evaluated the sensitivity to bispecific VHH-induced cytotoxicity after prior CD40 stimulation. Whereas coculture with CD40L-expressing fibroblasts increased the resistance of primary CLL cells to the Bcl-2 inhibitor venetoclax, the CD40L-expressing fibroblasts had no effect on the susceptibility to Vγ9Vδ2 T cell–mediated cytotoxicity (**Fig. 4B**).

Because the CD40-specific VHH counteracted CD40 stimulation, we investigated whether CD40-mediated venetoclax resistance could be reverted by the bispecific VHH. The capacity to antagonize CD40 stimulation was retained in the bispecific format, and the bispecific VHH completely prevented upregulation of CD86 and CD95 (**Fig. 4C**). rmCD40L also increased the resistance of CLL cells to venetoclax, which was abrogated by the bispecific VHH (**Fig. 4D**). The decreased sensitivity to venetoclax upon CD40 stimulation was previously reported to result from Bcl-xL upregulation (32), and the bispecific VHH prevented Bcl-xL upre-

gulation upon CD40 stimulation (**Fig. 4E**). Similar to the monovalent CD40-specific VHHs, culture of CLL cells with the bispecific VHHs did not lead to upregulation of CD86 or CD95 (Supplementary Fig. S2B).

The bispecific anti-CD40-Vδ2 VHH activates patient-derived Vγ9Vδ2 T cells

We then assessed whether the bispecific VHH also activated patient-derived Vγ9Vδ2 T cells because we and others previously found dysfunction of Vγ9Vδ2 T cells in CLL patients (21, 47). Whereas culture of T cell–enriched PBMCs from CLL patients with aminobisphosphonates led to activation of a minority of Vγ9Vδ2 T cells, a significantly higher proportion of Vγ9Vδ2 T cells producing IFNγ, TNF, and IL2 was noted in the presence of the bispecific VHH ($n = 7$; **Fig. 4F**; Supplementary Fig. S2C). Vγ9Vδ2 T cells from CLL patients also degranulated to a greater extent upon culture in the

presence of the bispecific VHH than in the presence of aminobisphosphonates (**Fig. 4G**). We then tested whether the bispecific VHH could also induce CLL lysis by autologous Vγ9Vδ2 T cells, by culturing purified CD3^{+} cells and CLL cells from the same donor together in the presence or absence of the bispecific VHH. The CD40-directed Vγ9Vδ2 T cells were also capable of lysis of autologous CLL cells (*n* = 5; **Fig. 4H**). The cytotoxic response mediated by Vγ9Vδ2 T cells was already observed at low effector-to-target (E:T) ratios of ±1:20, and as expected increased with a higher E:T ratio of ±1:5.

We then studied whether activation of Vγ9Vδ2 T cells induced by the bispecific VHH also induced expansion of Vγ9Vδ2 T cells. Culture of PBMCs for 1 week with the bispecific VHH led to enrichment of Vγ9Vδ2 T cells, with the proportion of Vγ9Vδ2 T cells within the total T-cell pool increasing on average 7.2-fold with the VHH in comparison with IL2 alone (*n* = 5; **Fig. 4I**). In summary, patient-derived Vγ9Vδ2 T cells were activated by, and cytotoxic against, autologous CLL cells in the presence of the bispecific VHH.

Activity of the bispecific VHH against primary MM

Because CD40 is also expressed on primary MM cells (ref. 26; representative histogram of four samples tested in **Fig. 5A**; mean geometric MFI: 7,794 ± 4,498 SD) and CD40 stimulation exerts various biological effects in this context, including proliferation of MM cells, we assessed the antitumor efficacy of the bispecific VHH in primary BM mononuclear cells from MM patients in two concentrations due to limitations in availability of patient material. When cultured overnight in the presence of the bispecific VHH, healthy donor–derived Vγ9Vδ2 T cells also lysed primary MM cells (*n* = 5; **Fig. 5B**). Vγ9Vδ2 T cells present in the BM of these patients were triggered to produce the proinflammatory cytokines IFNγ and TNF upon culture with the bispecific VHH (*n* = 6; **Fig. 5C** and **D**), as well as IL2 (Supplementary Fig. S2D). Similarly, Vγ9Vδ2 T cells present in BM mononuclear cells from MM patients degranulated after culture with the bispecific VHH (**Fig. 5D**). Together, these results indicated that the bispecific VHH was active against primary MM and could activate autologous BM–derived Vγ9Vδ2 T cells.

The bispecific VHH delays tumor outgrowth in a xenograft model

To study the effects of the bispecific VHH on tumor growth *in vivo*, immunodeficient NSG mice were injected with human MM-derived MM.1s cells. The tumor cells were allowed to grow out and engraft for 1 week before mice received the first of three weekly i.v. injections with either human Vγ9Vδ2 T cells or PBS, followed by twice weekly i.p. injections with the bispecific VHH or PBS, and the mice were sacrificed at the time of severe disease symptoms (**Fig. 6A**). Neither the bispecific VHH alone nor the Vγ9Vδ2 T cells alone significantly improved overall survival. In contrast, mice treated with both the bispecific VHH and Vγ9Vδ2 T cells lived significantly longer, with a median overall survival of 80 days versus 47 days in the control group (**Fig. 6B**). Mice treated with both the bispecific VHH and Vγ9Vδ2 T cells retained their initial body weight after 7 weeks of treatment (**Fig. 6C**). Human Vγ9Vδ2 T cells were infrequent or undetectable in the PB after 50 days of treatment, as well as in the BM and plasmacytomas at the time of sacrifice (Supplementary Fig. S3A and S3B). In conclusion, the bispecific VHH improved survival in a MM *in vivo* model.

Discussion

Vγ9Vδ2 T cells are endowed with intrinsic antitumor properties, predict favorable outcome, and can mount a cytotoxic response against various malignancies *in vitro*, including against CLL and MM cells (21, 22, 47–49). The therapeutic potential and safety of Vγ9Vδ2 T cell–based therapy in hematologic and solid malignancies have been established in clinical trials using adoptive transfer, although clinical results so far lack consistency (23–25, 50–52). CD40 is expressed on the surface of various solid (e.g., pancreatic cancer) and hematologic malignancies, including CLL and MM, and has an important role in mediating survival signaling and resistance to proapoptotic drugs (26, 28, 33, 37). The expression of CD40 on nonmalignant cells (e.g., antigen-presenting cells, pancreas; refs. 53, 54) poses a potential risk of on-target, off-tumor toxicity, although prior trials with both anti-CD40 antagonistic and agonistic monoclonal antibodies indicate the safety and tolerability of such approaches (38, 39). The safety of a
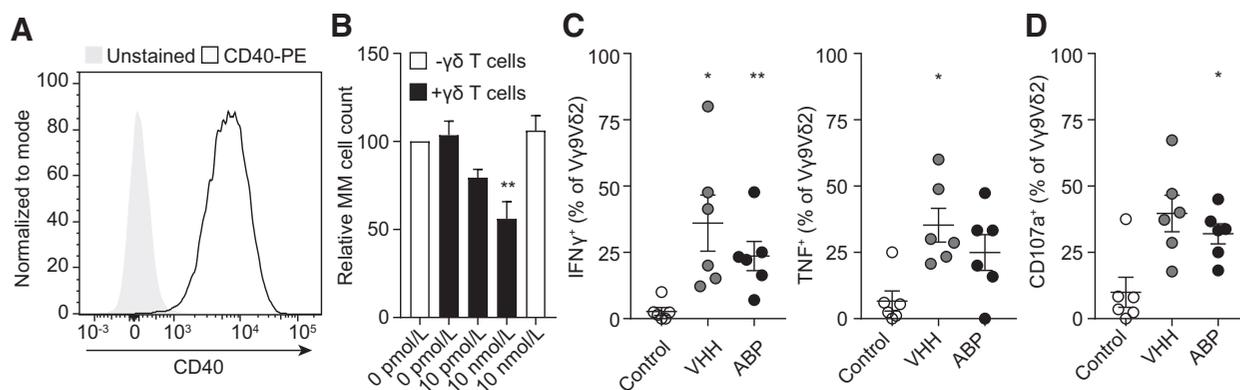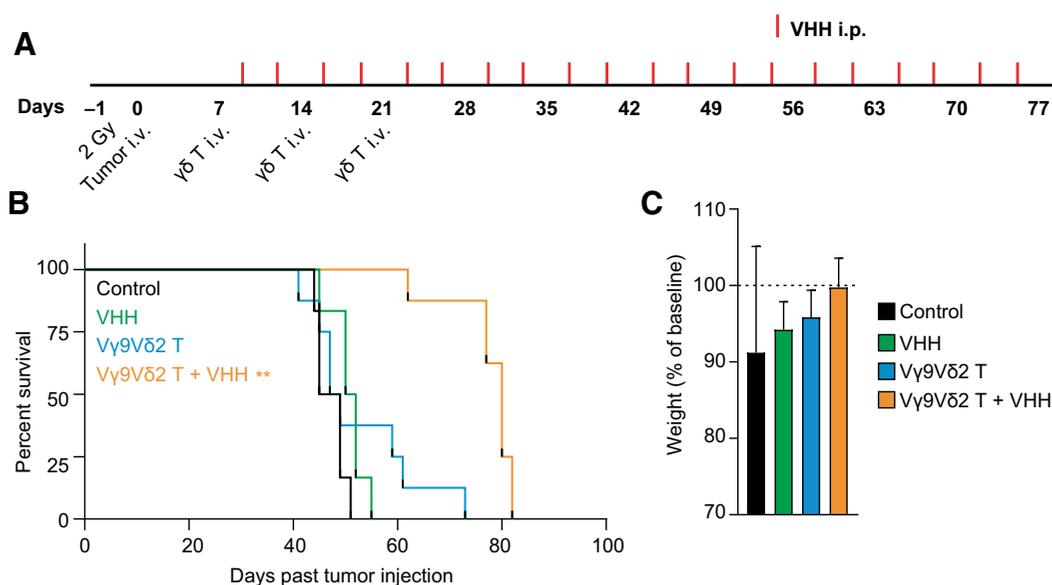

Figure 5.
The bispecific anti-CD40-Vδ2 VHH is active against primary MM. **A,** CD40 expression on primary MM cells. Representative histogram of four donors tested. **B,** BM of MM patients was cultured overnight in the presence or absence of healthy donor–derived Vγ9Vδ2 T cells in a 1:1 (Vγ9Vδ2-T:plasma cell) ratio in the presence of the bispecific VHH V19-5C8 (10 pmol/L or 10 nmol/L). Live plasma cells were quantified by flow cytometry using counting beads (*n* = 5). **C** and **D,** Mononuclear cells from the BM of MM patients were cultured overnight with V19-5C8 (10 nmol/L), aminobisphosphonate (ABP; 10 μmol/L zoledronic acid), or medium control in the presence of Brefeldin A, GolgiStop, and anti-CD107a to measure cytokine production (**C**) and degranulation (**D**) by flow cytometry (*n* = 6). Data, mean and SEM. *, *P* < 0.05; **, *P* < 0.01. **B–D,** Repeated-measures one-way ANOVA followed by Dunnett *post hoc* test compared with conditions without VHH.

Figure 6.
The bispecific anti-CD40-Vδ2 VHH prolongs survival *in vivo*. Immunodeficient mice were irradiated on day −1 and grafted (i.v.) with 2.5×10^6 MM.1s cells on day 0. Mice received PBS or human Vγ9Vδ2 T cells (1×10^7 cells; i.v.) on days 7, 14, and 21, followed by PBS or V19-5C8 (5 μg per mouse; i.p.) twice weekly starting on day 9. **A,** Schematic overview of treatment schedule. **B,** Kaplan–Meier analyses of mouse survival (control: $n = 6$; bispecific VHH: $n = 6$; Vγ9Vδ2 T cells: $n = 8$; bispecific VHH + Vγ9Vδ2 T cells: $n = 8$). **C,** Body weight after 7 weeks of treatment relative to individual body weight at time of tumor injection. **, $P < 0.01$. Data, mean and SD. **B,** Mantel–Cox log-rank test followed by Holm–Šidák *post hoc* test.

bispecific CD40-Vδ2 VHH will ultimately need to be assessed in early-phase clinical trials.

Here, we designed a strategy to activate Vγ9Vδ2 T cells in the presence of leukemic cells by constructing a bispecific VHH directed against CD40 and the Vγ9Vδ2 TCR. Previously, a Vδ2-specific VHH was selected from a generated panel of Vγ9- and Vδ2-TCR–specific VHHs to allow for more specific binding to phosphoantigen-responsive Vγ9Vδ2 T cells, based on the knowledge that a variable but sometimes considerable proportion of Vγ9^{+} cells pairs with a δ-chain other than Vδ2, whereas nearly all Vδ2^{+} cells coexpress the Vγ9 chain (55, 56). We generated three distinct CD40-specific antibodies that, when incorporated in a bispecific VHH format, induced potent Vγ9Vδ2 T cell–dependent lysis of leukemic cells *in vitro*. The V15- and V19-specific antibodies had a superior cytotoxic effect in comparison with V12. Both of these constructs prevented CD40L-induced survival of CLL cells. Although the two antibodies had comparable characteristics, the slightly stronger induction of cytotoxicity and blockade of CD40 stimulation favored further exploration of the V19-based antibody. The bispecific V19-5C8 VHH induced Vγ9Vδ2 T-cell degranulation upon exposure to CD40^{+} target cells. Although CD40 stimulation decreases the apoptotic sensitivity of CLL cells through Bcl-xL and Bfl-1 upregulation (32, 33), CD40 stimulation did not hamper bispecific VHH-induced cytotoxicity. The bispecific VHH also promoted the production of proinflammatory cytokines by Vγ9Vδ2 T cells, which, in combination with their antigen-presenting capacity (57, 58), may lead to the recruitment of other immune effector cells to initiate and propagate an antitumor response. The ability of the bispecific VHH to induce an antitumor response was further confirmed in a xenograft model. Adoptive transfer of human Vγ9Vδ2 T cells only resulted in significant prolongation of survival of mice engrafted with MM cells when combined with treatment with the bispecific VHH. The

limited persistence of human Vγ9Vδ2 T cells in immunodeficient mouse models that we and others have seen presumably led to cessation of the therapeutic effect (41, 59).

We demonstrated that the bispecific VHH had a dual mechanism of action, as it not only induced Vγ9Vδ2 T cell–mediated lysis, but also abrogated CD40 stimulation in CLL cells. Apart from the direct effect on CLL viability, CD40 stimulation induces concurrent resistance to fludarabine- and venetoclax-based treatment through NFκB signaling and subsequent upregulation of Bcl-xL, Bfl-1, and Mcl-1 (32–35). We showed that the bispecific VHH reversed CD40-induced upregulation of Bcl-xL and resistance to venetoclax, indicating that the bispecific VHH described here may increase the efficacy of venetoclax-based treatment. Because CD40/CD40L signaling also promotes survival and proliferation in lymphoma and MM cells, the CD40 antagonistic activity of the bispecific VHH also holds promise in other B-cell malignancies (37, 60, 61).

The application of bispecific constructs in T cell–based therapy allows flexible timing and dosing. In contrast, the administration of living cellular products such as CAR T-cell treatment restrains possibilities to adjust dosing or discontinuation in case of toxicity or refractory disease (62, 63). Bispecific constructs obviate the risk of genetically introducing therapy-specific resistance associated with CAR T-cell therapy (64). The low immunogenicity risk profile, good manufacturability, and stability of VHHs favor their use over constructs derived from conventional antibodies (40, 65).

We and others have previously described dysfunction of αβ T cells and Vγ9Vδ2 T cells in CLL patients, which could hamper the efficacy of autologous T cell–based therapy, and presumably results at least in part from impaired synapse formation (21, 47, 66, 67). Bispecific T cell–activating antibodies effectively induce immune synapse formation, particularly if the target epitope is proximal to the membrane, as is the case with relatively small target molecules such as CD40 (50

kDa; refs. 68, 69). Whether the bispecific Vγ9Vδ2 T-cell engager also improves synapse formation in CLL-derived Vγ9Vδ2 T cells remains to be studied. Our results, however, did demonstrate that the bispecific VHH was capable of activating patient-derived Vγ9Vδ2 T cells and enabled lysis of autologous tumor cells at low E:T ratios *ex vivo*. The bispecific VHH also induced Vγ9Vδ2 T-cell enrichment and could thereby result in an increase in the number of effector cells available. Novel agents such as venetoclax or ibrutinib are effective at reducing CLL burden, yet continuous treatment appears to be required. Because we and others have found indications that dysfunction of αβ T cells and Vγ9Vδ2 T cells is induced by CLL cells directly (21, 66), this suggested that the bispecific VHH could be useful in a consolidation setting, after prior reduction of the CLL disease load (e.g., by venetoclax or ibrutinib). We have previously shown that ibrutinib favorably alters the cytokine production profile of Vγ9Vδ2 T cells (70).

In conclusion, we generated a CD40-specific Vγ9Vδ2 T cell–engaging construct with a dual mechanism of action. The bispecific VHH deprived leukemic cells of CD40L-induced prosurvival signaling and apoptotic resistance. The bispecific VHH also selectively triggered potent antitumor effector functions of Vγ9Vδ2 T cells against CD40$^+$ malignant cells, including CLL and MM cells, in patient-derived samples, as well as in an *in vivo* xenograft model. Because CD40 is expressed by a wide range of hematologic and solid malignancies, this underscores the potential for broader therapeutic application of this Vγ9Vδ2 T cell–based bispecific strategy.

Authors' Disclosures

Authors' Contributions

I. de Weerdt: Conceptualization, formal analysis, investigation, writing–original draft. **R. Lameris:** Conceptualization, formal analysis, investigation, writing–review and editing. **G.L. Scheffer:** Formal analysis, investigation, writing–review and editing. **J. Vree:** Formal analysis, investigation, writing–review and editing. **R. de Boer:** Formal analysis, investigation, writing–review and editing. **A.G. Stam:** Formal analysis, investigation, writing–review and editing. **R. van de Ven:** Formal analysis, investigation, writing–review and editing. **M.-D. Levin:** Resources, writing–review and editing. **S.T. Pals:** Resources, writing–review and editing. **R.C. Roovers:** Conceptualization, writing–review and editing. **P.W.H.I. Parren:** Conceptualization, writing–review and editing. **T.D. de Gruijl:** Conceptualization, writing–review and editing. **A.P. Kater:** Conceptualization, writing–review and editing. **H.J. van der Vliet:** Conceptualization, writing–original draft.

Acknowledgments

References

1. Jain N, O'Brien S. Targeted therapies for CLL: practical issues with the changing treatment paradigm. Blood Rev 2016;30:233–44.
2. Goldschmidt H, Ashcroft J, Szabo Z, Garderet L. Navigating the treatment landscape in multiple myeloma: which combinations to use and when? Ann Hematol 2019;98:1–18.
3. Dhakal B, Vesole DH, Hari PN. Allogeneic stem cell transplantation for multiple myeloma: is there a future? Bone Marrow Transplant 2016;51: 492–500.
4. van Gelder M, de Wreede LC, Bornhauser M, Niederwieser D, Karas M, Anderson NS, et al. Long-term survival of patients with CLL after allogeneic transplantation: a report from the European Society for Blood and Marrow Transplantation. Bone Marrow Transplant 2017;52:372–80.
5. Bair SM, Porter DL. Accelerating chimeric antigen receptor therapy in chronic lymphocytic leukemia: the development and challenges of chimeric antigen receptor T-cell therapy for chronic lymphocytic leukemia. Am J Hematol 2019; 94:S10–S17.
6. Brudno JN, Kochenderfer JN. Recent advances in CAR T-cell toxicity: mechanisms, manifestations and management. Blood Rev 2019;34:45–55.
7. Ding W, LaPlant BR, Call TG, Parikh SA, Leis JF, He R, et al. Pembrolizumab in patients with CLL and Richter transformation or with relapsed CLL. Blood 2017; 129:3419–27.
8. Jelinek T, Paiva B, Hajek R. Update on PD-1/PD-L1 inhibitors in multiple myeloma. Front Immunol 2018;9:2431.
9. Teachey DT, Rheingold SR, Maude SL, Zugmaier G, Barrett DM, Seif AE, et al. Cytokine release syndrome after blinatumomab treatment related to abnormal macrophage activation and ameliorated with cytokine-directed therapy. Blood 2013;121:5154–7.
10. Porter DL, Hwang WT, Frey NV, Lacey SF, Shaw PA, Loren AW, et al. Chimeric antigen receptor T cells persist and induce sustained remissions in relapsed refractory chronic lymphocytic leukemia. Sci Transl Med 2015;7:303ra139.
11. Turtle CJ, Hay KA, Hanafi LA, Li D, Cherian S, Chen X, et al. Durable molecular remissions in chronic lymphocytic leukemia treated with CD19-specific chimeric antigen receptor–modified T cells after failure of ibrutinib. J Clin Oncol 2017; 35:3010–20.
12. Geyer MB, Riviere I, Senechal B, Wang X, Wang Y, Purdon TJ, et al. Safety and tolerability of conditioning chemotherapy followed by CD19-targeted CAR T cells for relapsed/refractory CLL. JCI Insight 2019;5:e122627.
13. Duell J, Dittrich M, Bedke T, Mueller T, Eisele F, Rosenwald A, et al. Frequency of regulatory T cells determines the outcome of the T-cell-engaging antibody blinatumomab in patients with B-precursor ALL. Leukemia 2017;31:2181–90.
14. Boroughs AC, Larson RC, Choi BD, Bouffard AA, Riley LS, Schiferle E, et al. Chimeric antigen receptor costimulation domains modulate human regulatory T cell function. JCI Insight 2019;5:e126194.
15. Koristka S, Cartellieri M, Theil A, Feldmann A, Arndt C, Stamova S, et al. Retargeting of human regulatory T cells by single-chain bispecific antibodies. J Immunol 2012;188:1551–8.
16. Togashi Y, Shitara K, Nishikawa H. Regulatory T cells in cancer immunosuppression–implications for anticancer therapy. Nat Rev Clin Oncol 2019;16: 356–71.

17. Schild H, Mavaddat N, Litzenberger C, Ehrich EW, Davis MM, Bluestone JA, et al. The nature of major histocompatibility complex recognition by gamma delta T cells. Cell 1994;76:29–37.

18. Gober HJ, Kistowska M, Angman L, Jeno P, Mori L, De Libero G. Human T cell receptor gammadelta cells recognize endogenous mevalonate metabolites in tumor cells. J Exp Med 2003;197:163–8.

19. Tanaka Y, Morita CT, Tanaka Y, Nieves E, Brenner MB, Bloom BR. Natural and synthetic non-peptide antigens recognized by human gamma delta T cells. Nature 1995;375:155–8.

20. Harly C, Guillaume Y, Nedellec S, Peigne CM, Monkkonen H, Monkkonen J, et al. Key implication of CD277/butyrophilin-3 (BTN3A) in cellular stress sensing by a major human gammadelta T-cell subset. Blood 2012;120:2269–79.

21. de Weerdt I, Hofland T, Lameris R, Endstra S, Jongejan A, Moerland PD, et al. Improving CLL Vgamma9Vdelta2-T-cell fitness for cellular therapy by ex vivo activation and ibrutinib. Blood 2018;132:2260–72.

22. Cui Q, Shibata H, Oda A, Amou H, Nakano A, Yata K, et al. Targeting myeloma-osteoclast interaction with Vgamma9Vdelta2 T cells. Int J Hematol 2011;94:63–70.

23. Abe Y, Muto M, Nieda M, Nakagawa Y, Nicol A, Kaneko T, et al. Clinical and immunological evaluation of zoledronate-activated Vgamma9gammadelta T-cell-based immunotherapy for patients with multiple myeloma. Exp Hematol 2009;37:956–68.

24. Kunzmann V, Smetak M, Kimmel B, Weigang-Koehler K, Goebeler M, Birkmann J, et al. Tumor-promoting versus tumor-antagonizing roles of gammadelta T cells in cancer immunotherapy: results from a prospective phase I/II trial. J Immunother 2012;35:205–13.

25. Wilhelm M, Kunzmann V, Eckstein S, Reimer P, Weissinger F, Ruediger T, et al. Gammadelta T cells for immune therapy of patients with lymphoid malignancies. Blood 2003;102:200–6.

26. Pellat-Deceunynck C, Bataille R, Robillard N, Harousseau JL, Rapp MJ, Juge-Morineau N, et al. Expression of CD28 and CD40 in human myeloma cells: a comparative study with normal plasma cells. Blood 1994;84:2597–603.

27. Young LS, Eliopoulos AG, Gallagher NJ, Dawson CW. CD40 and epithelial cells: across the great divide. Immunol Today 1998;19:502–6.

28. Gruss HJ, Dower SK. Tumor necrosis factor ligand superfamily: involvement in the pathology of malignant lymphomas. Blood 1995;85:3378–404.

29. Unek T, Unek IT, Agalar AA, Sagol O, Ellidokuz H, Ertener O, et al. CD40 expression in pancreatic cancer. Hepatogastroenterology 2013;60:2085–93.

30. Clark EA. A short history of the B-cell-associated surface molecule CD40. Front Immunol 2014;5:472.

31. van Attekum MH, Eldering E, Kater AP. Chronic lymphocytic leukemia cells are active participants in microenvironmental cross-talk. Haematologica 2017;102:1469–76.

32. Thijssen R, Slinger E, Weller K, Geest CR, Beaumont T, van Oers MH, et al. Resistance to ABT-199 induced by microenvironmental signals in chronic lymphocytic leukemia can be counteracted by CD20 antibodies or kinase inhibitors. Haematologica 2015;100:e302–6.

33. Jayappa KD, Portell CA, Gordon VL, Capaldo BJ, Bekiranov S, Axelrod MJ, et al. Microenvironmental agonists generate de novo phenotypic resistance to combined ibrutinib plus venetoclax in CLL and MCL. Blood Adv 2017;1:933–46.

34. Pascutti MF, Jak M, Tromp JM, Derks IA, Remmerswaal EB, Thijssen R, et al. IL-21 and CD40L signals from autologous T cells can induce antigen-independent proliferation of CLL cells. Blood 2013;122:3010–9.

35. Tromp JM, Tonino SH, Elias JA, Jaspers A, Luijks DM, Kater AP, et al. Dichotomy in NF-kappaB signaling and chemoresistance in immunoglobulin variable heavy-chain-mutated versus unmutated CLL cells upon CD40/TLR9 triggering. Oncogene 2010;29:5071–82.

36. Tong AW, Seamour B, Chen J, Su D, Ordonez G, Frase L, et al. CD40 ligand-induced apoptosis is Fas-independent in human multiple myeloma cells. Leuk Lymphoma 2000;36:543–58.

37. Tai YT, Li X, Tong X, Santos D, Otsuki T, Catley L, et al. Human anti-CD40 antagonist antibody triggers significant antitumor activity against human multiple myeloma. Cancer Res 2005;65:5898–906.

38. Bensinger W, Maziarz RT, Jagannath S, Spencer A, Durrant S, Becker PS, et al. A phase 1 study of lucatumumab, a fully human anti-CD40 antagonist monoclonal antibody administered intravenously to patients with relapsed or refractory multiple myeloma. Br J Haematol 2012;159:58–66.

39. Byrd JC, Kipps TJ, Flinn IW, Cooper M, Odenike O, Bendiske J, et al. Phase I study of the anti-CD40 humanized monoclonal antibody lucatumumab (HCD122) in relapsed chronic lymphocytic leukemia. Leuk Lymphoma 2012;53:2136–42.

40. Arbabi-Ghahroudi M. Camelid single-domain antibodies: historical perspective and future outlook. Front Immunol 2017;8:1589.

41. de Bruin RCG, Veluchamy JP, Lougheed SM, Schneiders FL, Lopez-Lastra S, Lameris R, et al. A bispecific nanobody approach to leverage the potent and widely applicable tumor cytolytic capacity of Vgamma9Vdelta2-T cells. Oncoimmunology 2017;7:e1375641.

42. McMillin DW, Delmore J, Negri JM, Vanneman M, Koyama S, Schlossman RL, et al. Compartment-specific bioluminescence imaging platform for the high-throughput evaluation of antitumor immune function. Blood 2012;119:e131–8.

43. Hallaert DY, Jaspers A, van Noesel CJ, van Oers MH, Kater AP, Eldering E. c-Abl kinase inhibitors overcome CD40-mediated drug resistance in CLL: implications for therapeutic targeting of chemoresistant niches. Blood 2008;112:5141–9.

44. de Bruin RCG, Lougheed SM, van der Kruk L, Stam AG, Hooijberg E, Roovers RC, et al. Highly specific and potently activating Vgamma9Vdelta2-T cell specific nanobodies for diagnostic and therapeutic applications. Clin Immunol 2016;169:128–38.

45. Masterson AJ, Sombroek CC, De Gruijl TD, Graus YM, van der Vliet HJ, Lougheed SM, et al. MUTZ-3, a human cell line model for the cytokine-induced differentiation of dendritic cells from CD34+ precursors. Blood 2002;100:701–3.

46. Roovers RC, Laeremans T, Huang L, De Taeye S, Verkleij AJ, Revets H, et al. Efficient inhibition of EGFR signaling and of tumour growth by antagonistic anti-EFGR nanobodies. Cancer Immunol Immunother 2007;56:303–17.

47. Coscia M, Vitale C, Peola S, Foglietta M, Rigoni M, Griggio V, et al. Dysfunctional Vgamma9Vdelta2 T cells are negative prognosticators and markers of dysregulated mevalonate pathway activity in chronic lymphocytic leukemia cells. Blood 2012;120:3271–9.

48. Gentles AJ, Newman AM, Liu CL, Bratman SV, Feng W, Kim D, et al. The prognostic landscape of genes and infiltrating immune cells across human cancers. Nat Med 2015;21:938–45.

49. Tosolini M, Pont F, Poupot M, Vergez F, Nicolau-Travers ML, Vermijlen D, et al. Assessment of tumor-infiltrating TCRVgamma9Vdelta2 gammadelta lymphocyte abundance by deconvolution of human cancers microarrays. Oncoimmunology 2017;6:e1284723.

50. Bennouna J, Bompas E, Neidhardt EM, Rolland F, Philip I, Galea C, et al. Phase-I study of Innacell gammadelta, an autologous cell-therapy product highly enriched in gamma9delta2 T lymphocytes, in combination with IL-2, in patients with metastatic renal cell carcinoma. Cancer Immunol Immunother 2008;57:1599–609.

51. Bennouna J, Lang I, Valladares-Ayerbes M, Boer K, Adenis A, Escudero P, et al. A phase II, open-label, randomised study to assess the efficacy and safety of the MEK1/2 inhibitor AZD6244 (ARRY-142886) versus capecitabine monotherapy in patients with colorectal cancer who have failed one or two prior chemotherapeutic regimens. Invest New Drugs 2011;29:1021–8.

52. Meraviglia S, Eberl M, Vermijlen D, Todaro M, Buccheri S, Cicero G, et al. In vivo manipulation of Vgamma9Vdelta2 T cells with zoledronate and low-dose interleukin-2 for immunotherapy of advanced breast cancer patients. Clin Exp Immunol 2010;161:290–7.

53. Banchereau J, Bazan F, Blanchard D, Briere F, Galizzi JP, van Kooten C, et al. The CD40 antigen and its ligand. Annu Rev Immunol 1994;12:881–922.

54. Vosters O, Beuneu C, Nagy N, Movahedi B, Aksoy E, Salmon I, et al. CD40 expression on human pancreatic duct cells: role in nuclear factor-kappa B activation and production of pro-inflammatory cytokines. Diabetologia 2004;47:660–8.

55. Davey MS, Willcox CR, Joyce SP, Ladell K, Kasatskaya SA, McLaren JE, et al. Clonal selection in the human Vdelta1 T cell repertoire indicates gamma-delta TCR-dependent adaptive immune surveillance. Nat Commun 2017;8:14760.

56. Davey MS, Willcox CR, Hunter S, Kasatskaya SA, Remmerswaal EBM, Salim M, et al. The human Vdelta2(+) T-cell compartment comprises distinct innate-like Vgamma9(+) and adaptive Vgamma9(−) subsets. Nat Commun 2018;9:1760.

57. Brandes M, Willimann K, Bioley G, Levy N, Eberl M, Luo M, et al. Cross-presenting human gammadelta T cells induce robust CD8+ alphabeta T cell responses. Proc Natl Acad Sci U S A 2009;106:2307–12.

58. Brandes M, Willimann K, Moser B. Professional antigen-presentation function by human gammadelta T Cells. Science 2005;309:264–8.

59. Kabelitz D, Wesch D, Pitters E, Zoller M. Characterization of tumor reactivity of human V gamma 9V delta 2 gamma delta T cells in vitro and in SCID mice in vivo. J Immunol 2004;173:6767–76.

60. Travert M, Ame-Thomas P, Pangault C, Morizot A, Micheau O, Semana G, et al. CD40 ligand protects from TRAIL-induced apoptosis in follicular lymphomas through NF-kappaB activation and up-regulation of c-FLIP and Bcl-xL. J Immunol 2008;181:1001–11.

61. Andersen NS, Larsen JK, Christiansen J, Pedersen LB, Christophersen NS, Geisler CH, et al. Soluble CD40 ligand induces selective proliferation of lymphoma cells in primary mantle cell lymphoma cell cultures. Blood 2000;96:2219–25.

62. Maude SL, Laetsch TW, Buechner J, Rives S, Boyer M, Bittencourt H, et al. Tisagenlecleucel in children and young adults with B-cell lymphoblastic leukemia. N Engl J Med 2018;378:439–48.

63. Neelapu SS, Locke FL, Bartlett NL, Lekakis LJ, Miklos DB, Jacobson CA, et al. Axicabtagene ciloleucel CAR T-cell therapy in refractory large B-cell lymphoma. N Engl J Med 2017;377:2531–44.

64. Ruella M, Xu J, Barrett DM, Fraietta JA, Reich TJ, Ambrose DE, et al. Induction of resistance to chimeric antigen receptor T cell therapy by transduction of a single leukemic B cell. Nat Med 2018;24:1499–503.

65. Perez JM, Renisio JG, Prompers JJ, van Platerink CJ, Cambillau C, Darbon H, et al. Thermal unfolding of a llama antibody fragment: a two-state reversible process. Biochemistry 2001;40:74–83.

66. Ramsay AG, Johnson AJ, Lee AM, Gorgun G, Le Dieu R, Blum W, et al. Chronic lymphocytic leukemia T cells show impaired immunological synapse formation that can be reversed with an immunomodulating drug. J Clin Invest 2008;118: 2427–37.

67. Hoffmann JM, Schubert ML, Wang L, Huckelhoven A, Sellner L, Stock S, et al. Differences in expansion potential of naive chimeric antigen receptor T cells from healthy donors and untreated chronic lymphocytic leukemia patients. Front Immunol 2017;8:1956.

68. Li J, Stagg NJ, Johnston J, Harris MJ, Menzies SA, DiCara D, et al. Membrane-proximal epitope facilitates efficient T cell synapse formation by anti-FcRH5/CD3 and is a requirement for myeloma cell killing. Cancer Cell 2017;31:383–95.

69. Hoffmann SC, Wabnitz GH, Samstag Y, Moldenhauer G, Ludwig T. Functional analysis of bispecific antibody (EpCAMxCD3)-mediated T-lymphocyte and cancer cell interaction by single-cell force spectroscopy. Int J Cancer 2011; 128:2096–104.

70. de Weerdt I, Hofland T, de Boer R, Dobber JA, Dubois J, van Nieuwenhuize D, et al. Distinct immune composition in lymph node and peripheral blood of CLL patients is reshaped during venetoclax treatment. Blood Adv 2019;3: 2642–52.

AACR American Association for Cancer Research

Cancer Immunology Research

A Bispecific Antibody Antagonizes Prosurvival CD40 Signaling and Promotes V γ9Vδ2 T cell–Mediated Antitumor Responses in Human B-cell Malignancies

Iris de Weerdt, Roeland Lameris, George L. Scheffer, et al.

Updated version	Access the most recent version of this article at: doi:10.1158/2326-6066.CIR-20-0138
Supplementary Material	Access the most recent supplemental material at: http://cancerimmunolres.aacrjournals.org/content/suppl/2020/11/11/2326-6066.CIR-20-0138.DC1

Cited articles	This article cites 70 articles, 25 of which you can access for free at: http://cancerimmunolres.aacrjournals.org/content/9/1/50.full#ref-list-1

E-mail alerts	Sign up to receive free email-alerts related to this article or journal.
Reprints and Subscriptions	To order reprints of this article or to subscribe to the journal, contact the AACR Publications Department at pubs@aacr.org.
Permissions	To request permission to re-use all or part of this article, use this link http://cancerimmunolres.aacrjournals.org/content/9/1/50. Click on "Request Permissions" which will take you to the Copyright Clearance Center's (CCC) Rightslink site.